

Supplemental Information for

Scanning transmission X-ray microscopy studies of electrochemical activation and capacitive behavior of Mn_3O_4 supercapacitor electrodes

Wenjuan Yang,^{1&} Haytham Eraky,^{2&} Chunyang Zhang,^{2,3} Adam P. Hitchcock² and Igor Zhitomirsky*

&these authors contributed equally

* corresponding author: zhitom@mcmaster.ca

CONTENTS

- S1 Results of sedimentation tests
- S2 Schematic of STXM
- S3 Spectral energy calibration
- S4 Analysis of impedance spectroscopy data using equivalent circuit
- S5 Mn 2p spectra of MnO_2 and Mn_3O_4 compared to literature
- S6 Comparison of STXM and SGM spectra

Section S1. Results of sedimentation tests

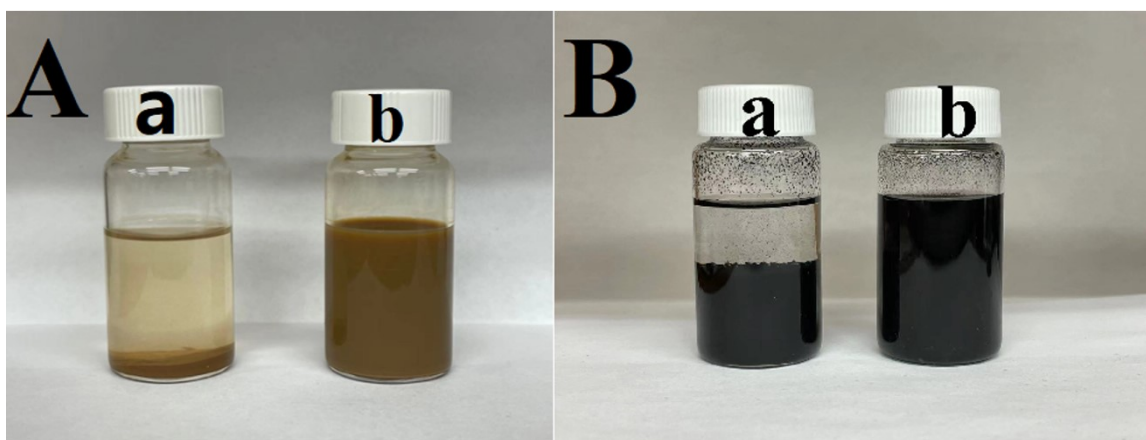


Figure S1. Suspensions of (A) Mn_3O_4 and (B) MWCNT, (a) without QC and (b) with QC as dispersants 7 days after preparation; mass ratio of QC: Mn_3O_4 and QC:MWCNT is 0.2.

Section S2. Schematic of STXM

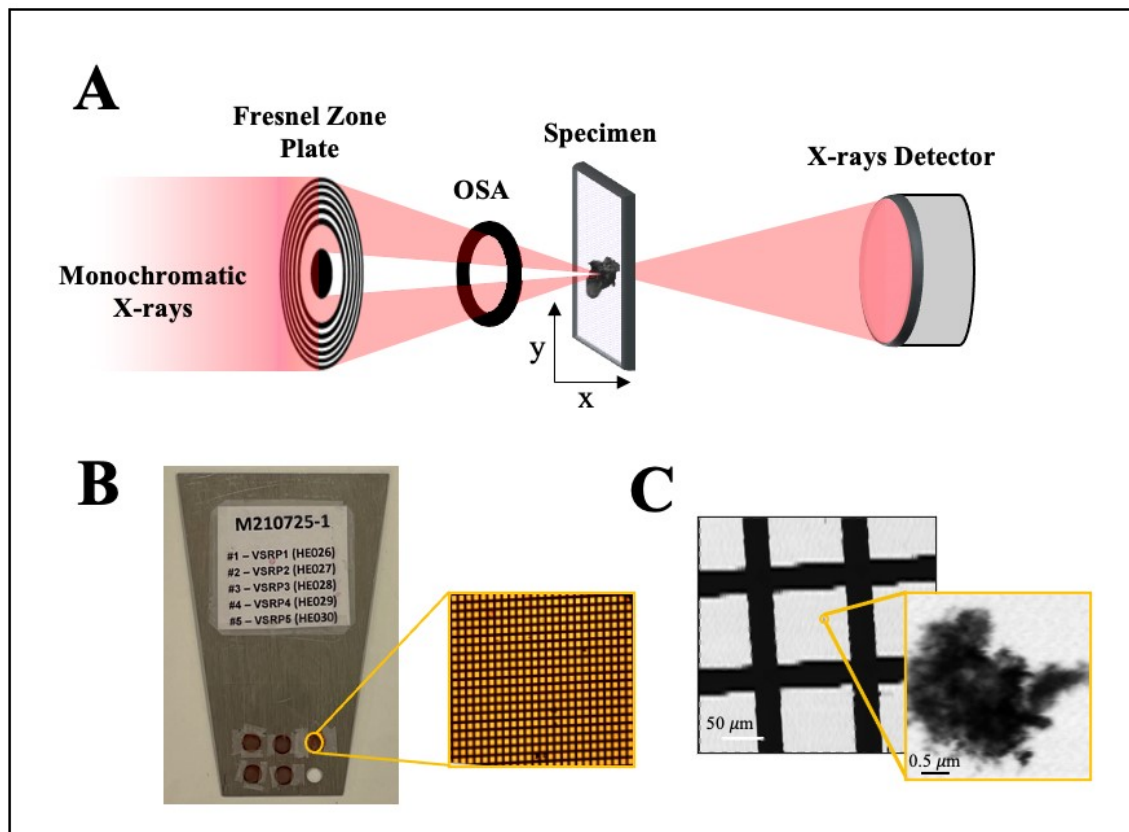


Figure S2. (A) Schematic diagram of scanning transmission x-ray microscopy (STXM), (B) samples on TEM grids mounted on STXM plate, (C) STXM image of the TEM grid square containing the measured region of the FSR1000 sample at 640 eV.

Figure S2A shows a schematic diagram of scanning transmission x-ray microscopy (STXM). Figure S2B shows VSRPs samples mounted on formvar coated TEM grids. Samples were prepared by attaching the TEM grid with a tape to the STXM plate, then drop-cast <1 mg powder on the support. This procedure was followed by tapping the edge of the STXM plate on a hard surface to detach weakly adhering particles. The TEM grid with remaining particles is then covered with a second TEM grid to avoid particles flying off the TEM grid due to sample charging when the X-ray beam hits the sample. Figure S-2C shows a STXM image of the TEM grid square containing the measured region of the FSR1000 sample.

Section S3. Spectral energy calibration

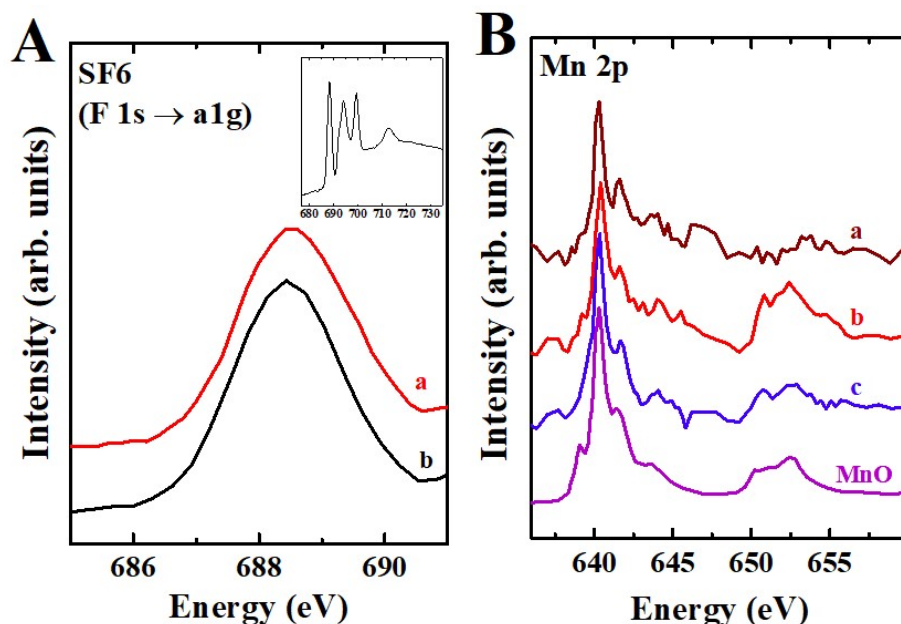


Figure S3. (A) $F\ 1s \rightarrow a_{1g}$ absorption peak of sulfur hexafluoride (SF_6) gas measured I (a) the I_o signal of a measurement of MnO_2 in the presence of SF_6 and, (b) at the hole (The inset shows the full $F\ 1s$ spectrum of SF_6 gas [s1]). (B) $Mn(II)$ signal present in the I_o of $Mn\ 2p$ spectra measured in STXM and used to confirm the energy scale. (a) as-prepared Mn_3O_4 , (b) FSR 100 and (c) FSR1000 cycle samples, compared to the digitized spectrum of MnO [s2].

Table S1. $Mn\ 2p$ and $F\ 1s$ energy features of measured samples compared to reference spectra.

Sample	edge	peak position (eV)	ΔE (eV)
MnO_2	$F\ 1s\ (F\ 1s \rightarrow a_{1g})$	688.41	0.14
At the hole	$F\ 1s\ (F\ 1s \rightarrow a_{1g})$	688.42	0.15
$F\ 1s$ reference spectra ^{S1}	$F\ 1s\ (F\ 1s \rightarrow a_{1g})$	688.27	-
As-prepared Mn_3O_4	$Mn\ 2p\ (L_3)$	640.10	-
FSR100 cycle sample	$Mn\ 2p\ (L_3)$	640.23	-
FSR1000 cycle sample	$Mn\ 2p\ (L_3)$	641.10	-
MnO digitized spectra ^{S2}	$Mn\ 2p\ (L_3)$	640.28	-

In order to calibrate the spectrum of MnO_2 and other species, sulfur hexafluoride (SF_6) gas ($P = 5$ mbar) was introduced into the STXM tank and its $F\ 1s$ spectrum measured as part of $Mn\ 2p$ stack measurements. The $F\ 1s \rightarrow a_{1g}$ peak (688.27 eV)^{s1} is observed in the I_o signal of the measured $Mn\ 2p$ stacks. Shifts of up to 0.15 eV were observed in the position of the $F\ 1s \rightarrow a_{1g}$ absorption peak (see table S1) which were tracking some

irreproducibility of the beamline energy scale. These shifts were used to set the Mn 2p energy scale accurately. Additionally, during some measurements, Mn(II) signal was observed in the I_o spectrum (see Figure S3B). This arises from contamination of the STXM zone plate or exit window. This signal was used to validate the Mn 2p energy scale of the as-prepared Mn₃O₄ and samples FSR 100 and 1000 cycle samples. The main L₃ peak Mn 2p spectrum of the Mn(II) contamination occurred at 640.4 eV, after calibration with the SF₆ signal measured at the same time.

Section S4 Analysis of impedance spectroscopy data using equivalent circuit

Figure S4(A) shows experimental EIS data presented in a Nyquist plot and simulation data obtained using (B) equivalent circuit.

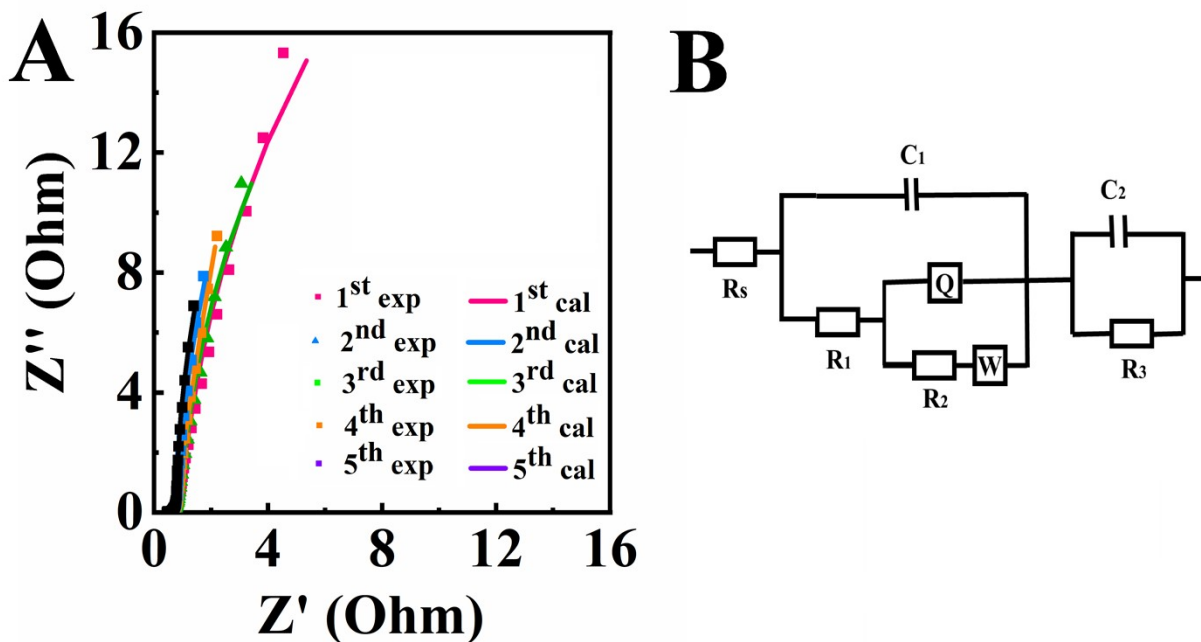


Figure S4. Nyquist plot of complex impedance for VSRPs 1-5: experimental data 1st exp-5th exp and simulation data 1st cal-5th cal, (B) equivalent circuit used for simulation.

The equivalent circuit was similar to that developed in a previous investigation (ref.³¹ in manuscript) for the analysis of porous electrodes with high active mass. The equivalent circuit contains R–C(Q) transmission line, Warburg impedance (W) and solution resistance R_s . In this circuit, capacitance (C) and constant phase element (Q) represented

double-layer capacitance at the electrode material -electrolyte interface and pseudocapacitance of the active material, respectively. C_2 and R_3 represent capacitance at the current collector-active material interface and charge transfer resistance, respectively. Simulation results showed that reduction of imaginary component of capacitance can be mainly attributed to increase in pseudocapacitance Q . The decrease of the real component resulted from the reduction of resistance of the transmission line.

Section S5. Comparison of Mn 2p spectra of MnO₂ and Mn₃O₄ with literature

Figure S5 compares the Mn 2p spectrum of MnO₂ we measured by STXM, with the Mn 2p spectra of MnO₂ reported by Gilbert et al.,^{s2} Toner et al.^{s3} and Stuckey et al.^{s4} The data plotted in figure S4 was digitized from the figures in these papers. Every effort was made to accurately reproduce the spectral shape and peak positions as reported in these papers. Gilbert et al.^{s2} report the sharp low lying peak in MnO₂ at 640.5 eV, while Toner et al.^{s3} report the corresponding peak at 639.3 eV, and Stuckey et al.^{s4} report the peak at 640.5 eV. Due to the presence of calibration signals above the Mn L signal (F 1s spectrum of SF₆), and exactly in the Mn L region (from the contaminant), we are confident our energy scale is accurate to within ± 0.1 eV. Here we are pointing out the existence of significant discrepancies in the energies of the Mn 2p spectrum of MnO₂ reported in the literature, We are preparing a more detailed evaluation of the soft X-ray NEXAFS spectroscopy of manganese oxides, which will be presented elsewhere.

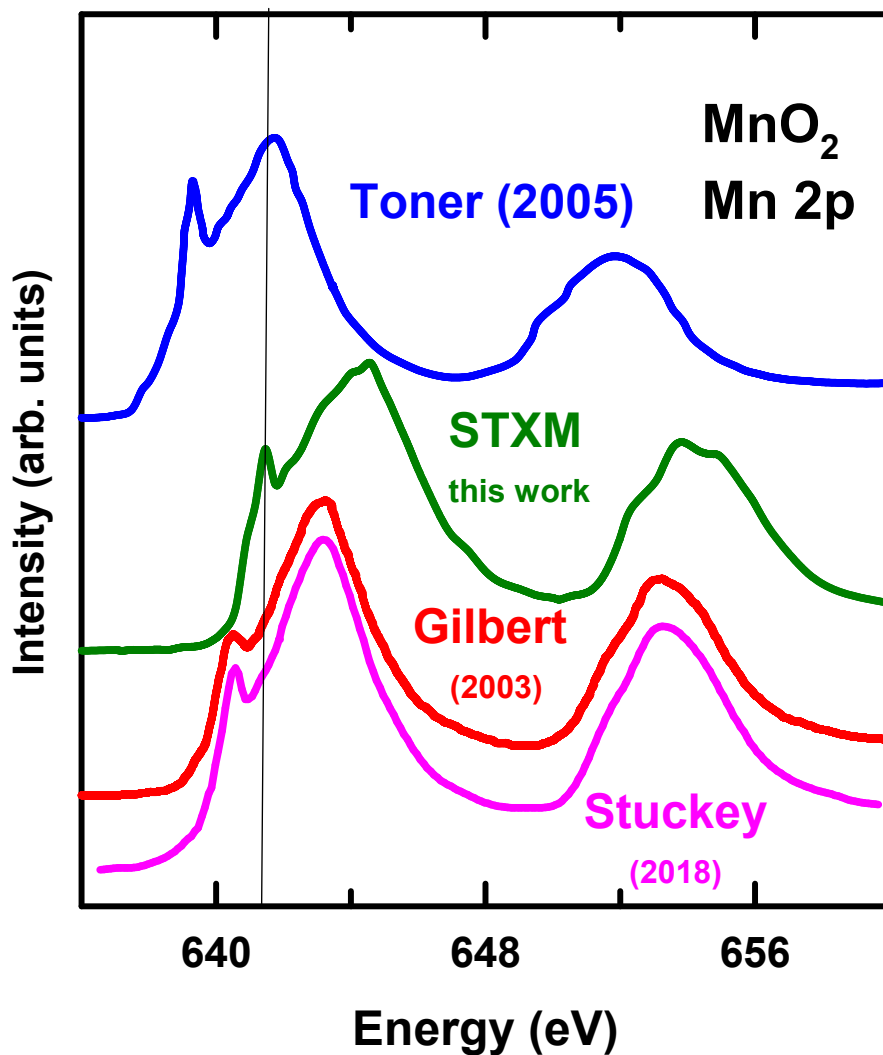


Figure S5 Comparison of the Mn 2p spectrum of MnO₂ from this work (STXM), with that reported in the literature by Gilbert et al.,^{s2} Toner et al.^{s3} and Stuckey et al.^{s4}

Figure S6 compares the Mn 2p spectrum of Mn₃O₄ reported by Gilbert et al.^{s2} and Stuckey et al.^{s4} with spectra of a commercial Mn₃O₄ sample, and of the as-prepared Mn(II,III) sample, that we measured by STXM. For the comparison shown in Fig. S6, the energy scale of each spectrum was set by assigning the position of the first Mn L₃ peak to 639.9 eV, which is that observed in the spectrum of the as-prepared Mn₃O₄. The digitized reference spectrum^{s2} and that of the as-prepared Mn₃O₄ previously measured showed the same Mn (L_{2,3}) features, indicating first L₃ sharp peak occurs at 639.9 eV. Although the main features of the Mn 2p spectrum of the commercial Mn₃O₄ sample

measured by TEY are present, the intensity of the first peak is considerably reduced, suggesting it is impure. For this reason we chose to use the spectra of the as-prepared material as the reference spectrum of Mn_3O_4 in the detailed analysis.

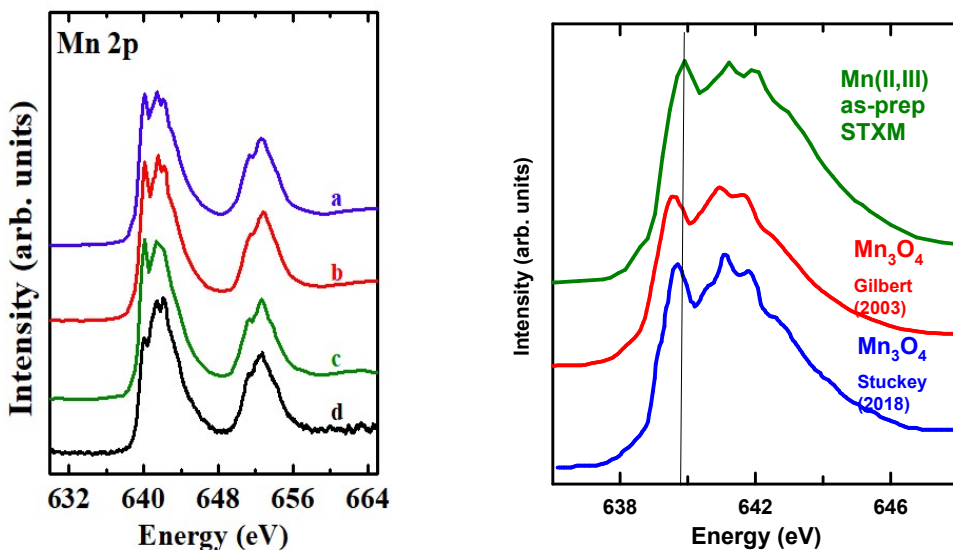


Figure S6. A. Mn_3O_4 (Mn 2p) absorption spectra of (a) as-prepared material, (b) digitized reference spectra from Gilbert et al.^{s2}, (c) previously measured Mn_3O_4 and (d) the SGM-TEY spectrum of commercial Mn_3O_4 (Sigma). B Expansion of the Mn L_3 region, comparing the spectrum of the as-prepared Mn(II,III) material with the spectra of Mn_3O_4 reported by Gilbert et al.,^{s2} and Stuckey et al.^{s4}

Section S6. Comparison of STXM and SGM spectra

Figure S7A and S6B present Mn $L_{2,3}$ and O 1s SGM spectra of the as-prepared Mn_3O_4 and MnO_2 reference spectra in comparison with measured spectra of VSRP1, VSRP3, VSRP5 and FSR1000 cycle samples. STXM and SGM spectra of the samples are presented in Figure S7C. The differences between SGM-TEY and STXM measurements might be related to the TEY spectra being dominated by the surface (sampling depth of ~ 5 -10 nm) while STXM is representative of the bulk (100-150 nm).

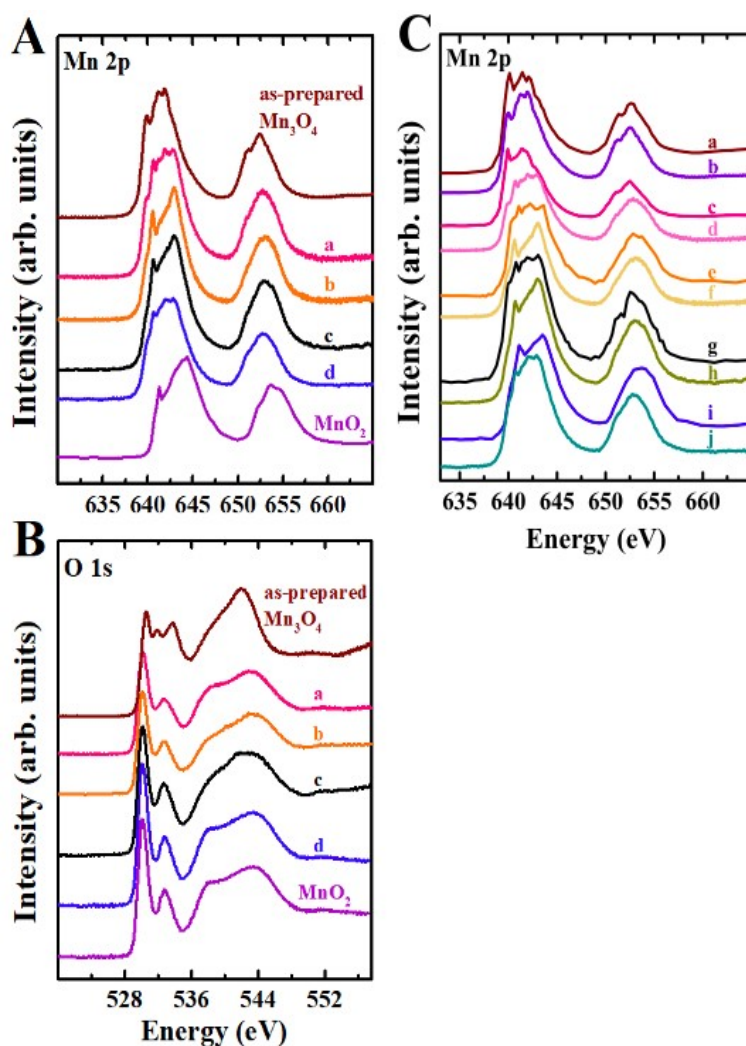


Figure S7. (A) Mn 2p, (B) O 1s SGM-TEY absorption spectra of (a) VSRP1, (b) VSRP3, (c) VSRP5 and (d) FSR1000 cycles, (C) shows comparison of STXM spectra (a), (c), (e), (g), (i) and SGM-TEY spectra, (b), (d), (f), (h), (j) of as-prepared Mn₃O₄, VSRP1, VSRP3, VSRP5 and FSR1000 cycles respectively.

References for SI

- S1. R.N.S. Sodhi & C.E. Brion, *J. Electron Spectroscopy & Rel. Phenom.* **34** 363 (1984).
 S2 B. Gilbert, B. Frazer, A. Belz, P. Conrad, K. Neilson, D. Haskel, J. Lang, G. Srajer and G. De Stasio, *The Journal of Physical Chemistry A* **107**, 2839 (2003)
 S3 B. Toner, S. Fakra, M. Villalobos, T. Warwick and G. Sposito, *Applied and environmental microbiology* **71**, 1300 (2005)
 S4 J. W. Stuckey, C. Goodwin, J. Wang, L.A. Kaplan, P. Vidal-Esquivel, T.P. Beebe Jr. and D.L. Sparks, *Geochem Trans* **19**, 6 (2018).